Spontaneous Hopf Fibration in the Two-Higgs-Doublet Model

R. A. Battye* and S. J. Cotterill†

Jodrell Bank Centre for Astrophysics, Department of Physics and Astronomy, University of Manchester, Manchester M13 9PL, United Kingdom

(Received 21 September 2023; revised 5 January 2024; accepted 9 January 2024; published 7 February 2024)

We show that energetic considerations enforce a Hopf fibration of the standard model topology within the 2HDM whose potential has either an SO(3) or U(1) Higgs-family symmetry. This can lead to monopole and vortex solutions. We find these solutions, characterize their basic properties and demonstrate the nature of the fibration along with the connection to Nambu's monopole solution. We point out that breaking of the $\mathrm{U(1)_{EM}}$ in the core of the defect can be a feature which leads to a nonzero photon mass there.

DOI: 10.1103/PhysRevLett.132.061601

Introduction.—The vacuum manifold of the standard model (SM) of particle physics is a three-sphere ($\mathcal{M} = S^3$) implying that there are no stable topological configurations in 3D since $\pi_2(\mathcal{M}) = I$, where $\pi_n(\mathcal{M})$ is the nth homotopy group of the manifold. However, there are interesting topological solutions with one unstable mode in 3D (sphalerons [1]) and 2D (electroweak vortices [2,3]) characterized by $\pi_3(\mathcal{M}) = Z$. Nambu suggested a monopolelike configuration [4] which can be understood via a local Hopf fibration $S^3 \cong S^2 \times S^1$ [5], which we discuss in more detail in Supplemental Material [6], such that $\pi_2(S^2 \times S^1) = Z$. However, this configuration is known to be unstable and, if it were to be realized, it would need to be combined with a string to form so-called "dumbbell" configurations [8,9]. The dynamics of such configurations has been linked with the production of primordial magnetic fields [10,11] and monopoles are being actively searched for in laboratory experiments [12].

We will discuss the two-Higgs doublet model (2HDM) [13]; in particular one where there are accidental symmetries. If the two doublets are Φ_1 and Φ_2 with $\Phi^T = (\Phi_1 \Phi_2)$ then the potential is given by $V(\Phi_1, \Phi_2) = V_2 + V_4$, where $V_2 = -\mu_1^2|\Phi_1|^2 - \mu_2^2|\Phi_2|^2$ and $V_4 = \lambda_1|\Phi_1|^4 + \lambda_2|\Phi_2|^4 + \lambda_3|\Phi_1|^2|\Phi_2|^2 + \lambda_4|\Phi_2^\dagger\Phi_1|^2$ which is $\mathrm{U(1)_{PQ}}$ symmetric. The symmetry can be enhanced to $\mathrm{SO(3)_{HF}}$ if $\mu_2 = \mu_1$, $\lambda_2 = \lambda_1$, and $\lambda_4 = 2\lambda_1 - \lambda_3$ [14,15].

The particle spectrum is well understood, for example [13,16]. There are five Higgs particles: two of which are CP even with masses M_h and M_H, a CP odd pseudoscalar with M_A and two charged Higgs particles with $M_{H_\pm}$. In the standard model alignment limit the h particle is that detected by experiments at the LHC and a wide range of measurements suggest that this limit should be close to being the case [17–21]. If there is a global $\mathrm{U(1)_{PQ}}$ symmetry then $M_A = 0$ and if this is extended to $\mathrm{SO(3)_{HF}}$ then in addition one has $M_H = 0$.

Topological defect solutions [22,23] associated with these symmetries were studied in detail in the context of the 2HDM in [15]. In particular, there can be domain wall [15,24–27], global vortex [15], and global monopole solutions [7]. Motivating the present study is the observation, based on field theory simulations from random initial conditions, that the vacuum is not neutral in the core of these defects [7,24,27] contrary to the assumption of [15]. We will see that this has profound implications. One should note that there are also several papers discussing nontopological configurations [28–31] and other compound structures of topological defects [32,33] (without any neutral vacuum violation) in the 2HDM that can be dynamically stable in certain regions of the parameter space. Here, we will focus purely only on topologically stabilized objects.

Accidental symmetries can be gauged using a covariant kinetic term

$$D_\mu\Phi = \left[(\sigma^0 \otimes \sigma^0)\partial_\mu + \frac{1}{2}ig(\sigma^0 \otimes \sigma^a)W_\mu^a + \frac{1}{2}ig'(\sigma^0 \otimes \sigma^0)Y_\mu + \frac{1}{2}ig''(\sigma^a \otimes \sigma^0)V_\mu^a\right]\Phi, \quad (1)$$

where $\sigma^\mu = (\sigma^0, \sigma^a)$ are the Pauli matrices including the identity. W_μ^a and Y_μ are the standard model gauge fields, with coupling constants g and g', respectively, and V_μ^a are the new gauge fields associated with the accidental symmetries with coupling constant g''—see Ref. [6] for more details on the symmetry transformations. For the purposes of this work, we set $g' = 0$ in order to simplify the defect

Published by the American Physical Society under the terms of the Creative Commons Attribution 4.0 International license. Further distribution of this work must maintain attribution to the author(s) and the published article's title, journal citation, and DOI. Funded by SCOAP³.

solutions, but note that we do not expect any changes in the qualitative features for nonzero g'.

Gauging the symmetries provides a natural mechanism for removing the Goldstone modes associated with the accidental symmetries allowing for a potentially viable model. In particular in the case of a $\mathrm{U(1)_{PQ}}$ symmetry the Goldstone mode with $M_A = 0$ becomes a massive gauge boson. There can be interesting models constructed with these symmetries, for example, models that can generate masses for neutrinos [34–36].

In this Letter, we will show that the Hopf fibration associated with the Nambu monopole is realized on energetic grounds within the 2HDM when there is either a $\mathrm{SO(3)_{HF}}$ or $\mathrm{U(1)_{PQ}}$ symmetry; something that we term "spontaneous Hopf fibration" (SHF). We will find monopole and vortex solutions for the case where the symmetries are gauged (although these can be easily adapted to the global limit).

Parametrizations and topology.—The eight fields of the 2HDM can be reparametrized as

$$\Phi = \frac{v_{\mathrm{SM}}}{\sqrt{2}} e^{(1/2)i\chi} \left(\sigma^0 \otimes U_L\right) \left(0 \;\; f_1 \;\; f_+ \;\; f_2 e^{i\xi}\right)^T, \quad (2)$$

using five fields $f_{1,2,+}$, ξ, and χ, and $U_L \in SU(2)_L$ which has 3 degrees of freedom. The constant $v_{\mathrm{SM}} = 246$ GeV is the standard model vacuum expectation value and $f_+ = 0$ corresponds to a neutral vacuum with zero photon mass. These degrees of freedom can also be encoded using bilinear forms, $R^\mu = \Phi^\dagger(\sigma^\mu \otimes \sigma^0)\Phi$, $n^a = -\Phi^\dagger(\sigma^0 \otimes \sigma^a)\Phi$ and $\tilde{R} = 2\Phi_2^T i\sigma^2 \Phi_1$, which are useful for understanding the topology of the vacuum manifold and the associated defects [7,15,37]. In particular, the neutral vacuum violation discovered in the core of defects in [7,24] can be traced by $R_+ = R_\mu R^\mu$, with $R_+ = 0$ corresponding to a neutral vacuum. One finds that two of the U_L degrees of freedom are encoded in $\hat{n}^a$, with the other associated with rotations about this axis, and the hypercharge degree of freedom U_Y is encoded in $\tilde{R} \propto \exp[i\chi]$. In contrast, R^μ is invariant under the standard model symmetries and contains the degrees of freedom that will, in general, change the potential. The R^0 component is $|\Phi|^2$ and so does not contribute to the topology of the vacuum manifold. The topological nontriviality of the vacuum manifold can, therefore, be most easily extracted by looking at the remaining three-vector R^a, which will contain all of the degrees of freedom associated with any additional symmetry transformations, U_H.

A notable difference between this topology and that of the 't Hooft-Polyakov monopole [38,39] and Nielsen-Olesen vortex [40] is that the topology lives in a space associated with these bilinear forms, rather than the fields themselves, which means that a half twist in field space can be topologically nontrivial and, in general, there is a factor of 2 difference between the topological degree of a field configuration and what one might naively expect. A consequence of this is that simple field configurations with unit winding often have discontinuities which must be resolved by the attachment of another soliton. It is for this reason that the Nambu monopole [4] has a string "emanating" from one of its poles.

In the $\mathrm{SO(3)_{HF}}$ case R^a only contributes to the potential with a term $\propto R^a R^a$, so rotations between the three components of R^a are a symmetry of the potential, generating an S^2 component of the vacuum manifold. Note that the topology is not S^3 as one might expect because U_H cannot perform rotations about R^a—this degree of freedom is already contained within U_L for rotations about n^a. Similarly, in the $\mathrm{U(1)_{PQ}}$ case, the R^3 component splits off from the other two but there remains a symmetry for rotations between R^1 and R^2, which is responsible for an S^1 direction. In general, there is an additional $S^1 \times S^3$ associated with the hypercharge and isospin symmetries because the degeneracy between U_Y and one of the directions in U_L is broken by f_+. Since this results in a massive photon, we avoid this scenario and choose the parameters so that $f_+ = 0$ in the vacuum, restoring the degeneracy so that the SM symmetries only contribute S^3. Therefore, the topology of the vacuum manifolds associated with the accidental symmetries are $\mathcal{M} = S^2 \times S^3$ for the case of $\mathrm{SO(3)_{HF}}$ and $\mathcal{M} = S^1 \times S^3$ for $\mathrm{U(1)_{PQ}}$ [15], which admit monopoles and vortices due to the nontrivial homotopy groups $\pi_2(S^2 \times S^3) = \mathbb{Z}$ and $\pi_1(S^1 \times S^3) = \mathbb{Z}$, respectively.

Monopole solutions.—In the $\mathrm{SO(3)_{HF}}$ symmetric model, using 3D spherical polar coordinates (r, θ, ϕ), we can construct the monopole ansatz for the scalar field [6,7]

$$\Phi(r,\theta,\phi) = \frac{v_{\mathrm{SM}}}{2\sqrt{2}} \begin{pmatrix} -(k+k_+)\sin\theta e^{-i\phi} \\ (k-k_+) + (k+k_+)\cos\theta \\ -(k-k_+) + (k+k_+)\cos\theta \\ (k+k_+)\sin\theta e^{i\phi} \end{pmatrix}, \quad (3)$$

where $k = k(r)$ and $k_+ = k_+(r)$ are functions constructed from $f_{1,2,+}$ that retain the ability to change the potential energy while the other degree of freedom (as well as ξ) is used to wind around the vacuum manifold. This ansatz has the property that $R^a = n^a = (k^2 - k_+^2)\hat{r}^a$. The feature $\hat{R}^a = \hat{r}^a$ is necessary for a monopole configuration with unit winding (or related to this by a homomorphism) and this structure, by itself, would give rise to a 2HDM equivalent of the Nambu monopole—with a divergence in the gradient energy that necessitates the emergence of a string from one of the poles. However, the isospin degrees of freedom, contained within U_L, can resolve this divergence when we also have that $\hat{n}^a = \hat{r}^a$, which gives the appearance of an underlying topological complexity in the structure of n^a, but it occurs for energetic reasons that are only indirectly topological. The degree of freedom associated with rotations about n^a contains no structure—only the possibility for global transformations—and it is this effect that we have termed SHF. The S^3 of the SM becomes $S^2 \times S^1$ with the S^2 part inheriting the same twists as the S^2 of the $\mathrm{SO(3)_{HF}}$ symmetry and the S^1 part containing nothing except possible global rotations.

For the gauge fields, we choose to work in the temporal gauge such that the time components of the gauge fields are zero and make the ansatz $gW_i^a = -(1/r)h(r)\epsilon^a{}_{ij}\hat{r}^j$ and $g''V_i^a = -(1/r)H(r)\epsilon^a{}_{ij}\hat{r}^j$. After the standard rescaling to reduce the number of significant parameters in the model by two, we find that the energy functional under this ansatz is

$$E = \frac{4\pi v_{\mathrm{SM}}}{g}\int r^2 dr\left\{\frac{1}{2}\left(\frac{dk}{dr}\right)^2 + \frac{1}{2}\left(\frac{dk_+}{dr}\right)^2 + \frac{1}{8r^2}(k+k_+)^2(h+H-2)^2 + \frac{1}{8r^2}(k-k_+)^2(h-H)^2 + \frac{1}{2r^2}\left[2\left(\frac{dh}{dr}\right)^2 + \frac{1}{r^2}h^2(2-h)^2\right] + \frac{1}{2\tilde{g}^2r^2}\left[2\left(\frac{dH}{dr}\right)^2 + \frac{1}{r^2}H^2(2-H)^2\right] + \frac{\tilde{\lambda}}{4}\left[(k^2+k_+^2-1)^2 - \zeta_4 k^2 k_+^2\right]\right\}, \tag{4}$$

where the remaining parameters are $\tilde{g} = g''/g$, $\tilde{\lambda} = \lambda/g^2$, and $\zeta_4 = \lambda_4/\lambda$. Neutral vacuum violation occurs when both k and k_+ are simultaneously nonzero and we choose, by convention, k_+ to be zero in the vacuum. We can perform a simple analysis (neglecting gradient energy contributions) to predict when there will be neutral vacuum violation in the core of the monopole by looking at the effective mass $m_{k_+}^2 = \lambda[2(k^2-1) - \zeta_4 k^2]/4$. If a monopole were to have $k_+ = 0$ everywhere, then the effective mass at the core of the monopole (where $k = 0$) would be $-(\tilde{\lambda}/2)$, which is always negative and independent of ζ_4. The presence of this negative mass term indicates that the energy would be reduced if $k_+ \neq 0$ and therefore we expect neutral vacuum violation to be a generic effect in the core of 2HDM monopoles.

In Fig. 1 we present the energy and $R_+(0)$ (fixing $v_{\mathrm{SM}} = 1$) as a function of the mass ratio $\epsilon = M_{H\pm}/M_h = \frac{1}{2}\sqrt{-\zeta_4}$ and we also show an example solution in the inset plot. As expected, for all values of ϵ presented here, there is neutral vacuum violation in the core of the monopole, although it decreases as ϵ grows and appears to be approaching zero, while conversely, the energy grows with ϵ and appears to be approaching a maximum. Perhaps the most noticeable feature of the solution is that $k + k_+ = 0$ at the center—in fact this is enforced by the gradient energy and is true for all values of ϵ. The effects of $\tilde{\lambda}$ can be broadly described as changing the length scale ratio between the scalar fields and the vector fields and, similarly, $\tilde{g}$ changes the length scale ratio between the two gauge fields.

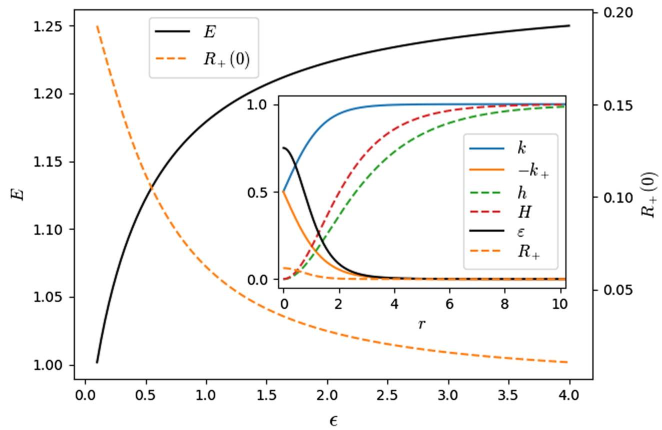

FIG. 1. The variation of E (black) and R_+ at the monopole core (dotted orange) as a function of the mass ratio ϵ, with the other parameters fixed to $\tilde{\lambda} = 1$ and $\tilde{g}^2 = 2$. The inset plot presents the field profiles of an example solution ($\epsilon = 1$) and also displays the energy density, ε, and R_+.

Vortex solutions.—In the $\mathrm{U(1)_{PQ}}$ symmetric case, using plane polar coordinates (r, θ), we can make the vortex ansatz $\Phi = \Phi(r, \theta)$ from Eq. (2) with $f_i = f_i(r)$ for $i = 1, 2, +$ and $\xi = \theta$ [6] which has a similar property to the monopole in that $\hat{R}^b = \hat{n}^b = \hat{r}^b$, where $b \in [1, 2]$, although now, unlike the monopole case, $n^b = 0$ in the vacuum. The remaining components are $R^3 = f_1^2 - f_+^2 - f_2^2$ and $n^3 = f_1^2 - f_+^2 + f_2^2$. We note that, in a similar way to the Nambu monopole solution, there is a stringlike configuration, characterized by $\pi_1(S^2 \times S^1) = Z$ and with structure only in R^b, where the divergence in the gradient energy is resolved by attaching a domain wall to one side. This is related to an unstable (due to the tension in the wall) configuration in the SM where $\hat{n}^b = \hat{r}^b$. Once again, for the 2HDM configuration, we can use the isospin rotations to resolve the divergence without the domain wall. The SHF acts here, again, to split $S^3 \to S^2 \times S^1$, but now it is the S^1 part that inherits the twists of the $\mathrm{U(1)_{PQ}}$.

Now we choose to make a gauge transformation that absorbs the phase winding of the scalar field into W_i^a and V_i^3 [the only new gauge field in the $\mathrm{U(1)_{PQ}}$ model] so that we can make the ansatz $gW_i^a = (1/r)\{h_1(r)\hat{x}^a + [1 - h_3(r)]\hat{z}^a\}\hat{\theta}_i + h_2(r)\hat{y}^a\hat{r}_i$ and $g''V_i^3 = (1/r)[1 - H(r)]\hat{\theta}_i$. Again, if we make the standard rescalings then we can express the energy per unit length of the string as

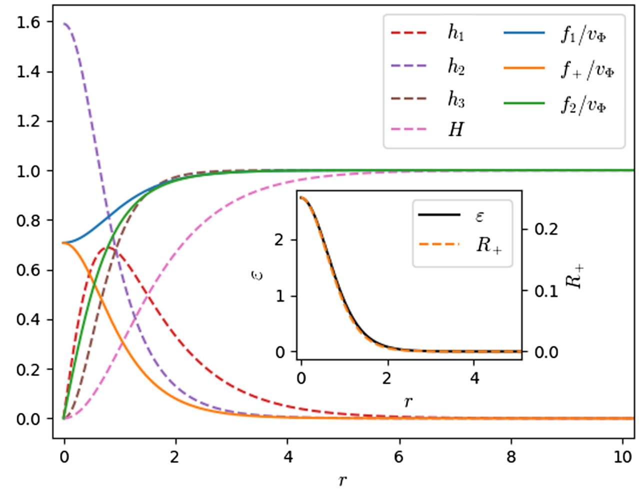

FIG. 2. The field profiles for a string solution with $\tilde{\lambda}_1 = 1$, $\tilde{g}^2 = 1$, $\tilde{\eta}^2 = 1$, $\zeta_2 = 1$, $\zeta_3 = -0.4$, and $\zeta_4 = -0.8$—the last four parameter choices corresponding to the alignment limit with $\epsilon = 1$, $\delta = 2$, $\tan\beta = 1$. The inset plot displays the energy density, ε, and R_+ for the same solution.

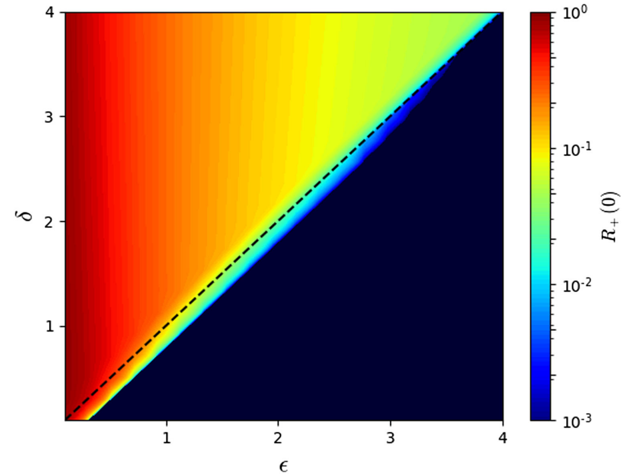

FIG. 3. A contour plot showing how R_+ at the string core varies with the mass ratios ϵ and δ in the alignment limit and with $\tilde{\lambda}_1 = \tilde{g}^2 = \tan\beta = 1$. Note that the dark blue color on most of the lower right region of the plot is off the bottom of the color scale—corresponding to a neutral vacuum.

$$
\begin{aligned}
E = 2\pi v_{\rm SM}^2 \eta_1^2 \int r dr \Bigg\{ & \frac{1}{2}\left(\frac{df_1}{dr}\right)^2 + \frac{1}{2}\left(\frac{df_+}{dr}\right)^2 + \frac{1}{2}\left(\frac{df_2}{dr}\right)^2 - \frac{1}{2} h_2 \left(f_+ \frac{df_2}{dr} - f_2 \frac{df_+}{dr}\right) + \frac{1}{8}\Bigg(\frac{h_1^2}{r^2} + h_2^2 \\
& + \frac{1}{r^2}(h_3 - H)^2\Bigg)(f_1^2 + f_+^2) - \frac{1}{2r^2} h_1 (1 - H) f_+ f_2 + \frac{1}{8}\left(\frac{h_1^2}{r^2} + h_2^2 + \frac{1}{r^2}(2 - h_3 - H)^2\right) f_2^2 + \frac{1}{2r^2}\Bigg[\left(\frac{dh_1}{dr}\right)^2 \\
& + \left(\frac{dh_3}{dr}\right)^2 - 2h_2\left(h_1 \frac{dh_3}{dr} + (1 - h_3)\frac{dh_1}{dr}\right) + h_1^2 h_2^2 + (1 - h_3)^2 h_2^2\Bigg] + \frac{1}{2\tilde{g}^2 r^2}\left(\frac{dH}{dr}\right)^2 + \frac{\tilde{\lambda}_1}{4}\Bigg[(f_1^2 - 1)^2 \\
& + \zeta_2 (f_+^2 + f_2^2 - \tilde{\eta}^2)^2 + \zeta_3 f_1^2 (f_+^2 + f_2^2) + \zeta_4 f_1^2 f_2^2\Bigg]\Bigg\}, \qquad (5)
\end{aligned}
$$

where $\tilde{g} = g''/g$, $\tilde{\eta} = \eta_2/\eta_1$, $\tilde{\lambda}_1 = \lambda_1/g^2$, and $\zeta_i = \lambda_i/\lambda_1$ so that the model is left with six parameters (η_i is defined by the relationship $\mu_i^2 = \lambda_i \eta_i^2 v_{\rm SM}^2$). We can perform an effective mass analysis here too, just as in the monopole case. The relevant effective mass is $m_{f_+}^2 = \tilde{\lambda}_1[2\zeta_2(f_2^2 - \tilde{\eta}^2) + \zeta_3 f_1^2]/4$ and if the string were to have $f_+ = 0$ everywhere, as well as $f_1(0) = 1$ and $f_2(0) = 0$, then this would take the value $\tilde{\lambda}_1[-2\zeta_2\tilde{\eta}^2 + \zeta_3]/4$, so the neutral vacuum violation in the core is not generic but depends upon the sign of $\zeta_3 - 2\zeta_2\tilde{\eta}^2$. Note that $f_2(0) = 0$ is enforced by the winding of the string but $f_1(0) = 1$ is an overly simplistic assumption, even if $f_+ = 0$ everywhere, so this approach will be less accurate for vortices than for the monopoles.

In Fig. 2 we present the field profiles of a string solution with a separate inset plot showing the energy density and R_+ for the same solution and in Fig. 3 we show how R_+, at the core of the string, varies with the mass ratios $\epsilon = M_{H\pm}/M_h$ and $\delta = M_H/M_h$, in the alignment limit and with $\tan\beta = 1$ (which sets the vacuum values of the fields so that $|\Phi_1|^2 = |\Phi_2|^2 = v_\Phi^2$). Note that we have rescaled $R_+ \to R_+/(v_\Phi v_{\rm SM})^4$ implicitly in these plots.

From the profiles we see that the solution has retained a feature that is similar to one observed for the monopole solutions, namely that $f_1 = f_+$ at the center. However, this is no longer guaranteed by the gradient energy and, in fact, is only an approximate equality that occurs in a subset of the parameter space. The parameters $\tilde{\lambda}_1$ and $\tilde{g}^2$ play a very similar role to the equivalent parameters from the monopole case but the other parameters have more complicated effects on the solutions that are difficult to broadly summarize in this way. From the contour plot we can see that there is a clear transition across the line which is approximately $\epsilon = \delta$, corresponding to $\zeta_3 = 2$. Because of our fixed parameter choices we have $\zeta_2 = \tilde{\eta}^2 = 1$ and therefore this is consistent with the behavior that we predicted from the effective mass analysis.

Discussion and conclusions.—The solutions that we have presented in this Letter are evidence of a new mechanism—that we have called "spontaneous Hopf fibration"—at work in the 2HDM. It allows for a topologically nontrivial subspace of the vacuum manifold to imprint itself onto another, topologically trivial section of the manifold. This results in solitons that appear to have topological structure in the SM degrees of freedom but, in fact, it is purely caused by energetics. The coupling between the S^3 of the SM to the rest of the vacuum manifold, in the gradient energy term, causes a Hopf fibration of the space $S^3 \to S^2 \times S^1$, with the appropriate component of this space taking on structure to match the winding around S^2 for monopoles and S^1 for strings.

In [7] we present evidence from simulations of the global 2HDM model in which stable monopoles form that have neutral vacuum violation in the cores and a structure in the bilinear vectors that is the same as what one would expect from the solutions presented here. In [6] we do the same for the case of strings. These simulations suggest that the solutions we have found are those most relevant to the study of topological defects in the 2HDM.

A phenomenologically relevant consequence of the SHF in the 2HDM is that it allows for the neutral vacuum condition to be violated inside the core of the defects, generating a nonzero mass for the photon. In the case of strings, this is dependent upon the choice of parameters, however in the monopole case it is predicted to always occur if the gradient energy contributions are neglected. The interaction between photons and superconducting defects has been analyzed in [41] for a toy model but this work has opened up the possibility for novel interactions between standard model particles and 2HDM defects which are deserving of more investigation. In [7] it was observed that the additional structure of global 2HDM monopoles did not affect the scaling of their number density, but other potential cosmological consequences warrant further studies of these defects.

We would like to conclude by emphasising that, although we have discussed SHF in the context of the 2HDM, we suggest that it could be a more general effect that can occur in other models that have vacuum manifolds constructed from coupled subspaces, when at least one of them is topologically nontrivial.

We would like to thank Jeff Forshaw for helpful comments on the phenomenological viability of these models. R. B. would like to thank Apostolos Pilaftsis, Gary Brawn, and Dominic Viatic for their collaboration on the 2HDM which ultimately lead to this work.

[*]richard.battye@manchester.ac.uk
[†]steven.cotterill@manchester.ac.uk

[1] F. R. Klinkhamer and N. S. Manton, Phys. Rev. D **30**, 2212 (1984).
[2] T. Vachaspati, Nucl. Phys. **B397**, 648 (1993).
[3] A. Achucarro and T. Vachaspati, Phys. Rep. **327**, 347 (2000).
[4] Y. Nambu, Nucl. Phys. **B130**, 505 (1977).
[5] G. W. Gibbons, M. E. Ortiz, F. Ruiz Ruiz, and T. M. Samols, Nucl. Phys. **B385**, 127 (1992).
[6] See Supplemental Material at http://link.aps.org/supplemental/10.1103/PhysRevLett.132.061601 for more detail on the Hopf fibration, symmetry transformations, ansatz construction, and simulations of strings, which includes Ref. [7].
[7] R. A. Battye, S. J. Cotterill, and D. G. Viatic, Phys. Lett. B **844**, 138091 (2023).
[8] G. Lazarides, Q. Shafi, and T. Vachaspati, Phys. Rev. D **104**, 035020 (2021).
[9] T. Patel and T. Vachaspati, Phys. Rev. D **107**, 093010 (2023).
[10] T. Vachaspati, Rep. Prog. Phys. **84**, 074901 (2021).
[11] T. Patel and T. Vachaspati, J. High Energy Phys. 01 (2022) 059.
[12] B. Acharya *et al.* (MoEDAL Collaboration), Nature (London) **602**, 63 (2022).
[13] G. C. Branco, P. M. Ferreira, L. Lavoura, M. N. Rebelo, M. Sher, and J. P. Silva, Phys. Rep. **516**, 1 (2012).
[14] P. M. Ferreira, H. E. Haber, and J. a. P. Silva, Phys. Rev. D **79**, 116004 (2009).
[15] R. A. Battye, G. D. Brawn, and A. Pilaftsis, J. High Energy Phys. 08 (2011) 020.
[16] A. Pilaftsis and C. E. M. Wagner, Nucl. Phys. **B553**, 3 (1999).
[17] A. Celis, V. Ilisie, and A. Pich, J. High Energy Phys. 12 (2013) 095.
[18] C.-W. Chiang and K. Yagyu, J. High Energy Phys. 07 (2013) 160.
[19] C.-Y. Chen, S. Dawson, and M. Sher, Phys. Rev. D **88**, 015018 (2013); **88**, 039901(E) (2013).
[20] D. Chowdhury and O. Eberhardt, J. High Energy Phys. 05 (2018) 161.
[21] J. Haller, A. Hoecker, R. Kogler, K. Mönig, T. Peiffer, and J. Stelzer, Eur. Phys. J. C **78**, 675 (2018).
[22] A. Vilenkin and E. Shellard, *Cosmic Strings and Other Topological Defects*, Cambridge Monographs on Mathematical Physics (Cambridge University Press, Cambridge, England, 1994).
[23] N. Manton and P. Sutcliffe, *Topological Solitons* (Cambridge University Press, Cambridge, England, 2004).
[24] R. A. Battye, A. Pilaftsis, and D. G. Viatic, J. High Energy Phys. 01 (2021) 105.
[25] R. A. Battye, A. Pilaftsis, and D. G. Viatic, Phys. Rev. D **102**, 123536 (2020).
[26] N. Chen, T. Li, Z. Teng, and Y. Wu, J. High Energy Phys. 10 (2020) 081.
[27] K. H. Law and A. Pilaftsis, Phys. Rev. D **105**, 056007 (2022).
[28] C. Bachas and T. N. Tomaras, Phys. Rev. Lett. **76**, 356 (1996).
[29] C. Bachas, B. Rai, and T. N. Tomaras, Phys. Rev. Lett. **82**, 2443 (1999).
[30] C. Bachas, P. Tinyakov, and T. Tomaras, Phys. Lett. B **385**, 237 (1996).
[31] M. A. Earnshaw and M. James, Phys. Rev. D **48**, 5818 (1993).
[32] M. Eto, Y. Hamada, M. Kurachi, and M. Nitta, J. High Energy Phys. 07 (2020) 004.
[33] M. Eto, Y. Hamada, and M. Nitta, J. High Energy Phys. 02 (2022) 099.
[34] P. Ko, Y. Omura, and C. Yu, Phys. Lett. B **717**, 202 (2012).

[35] D. Camargo, A. Dias, T. de Melo, and F. Queiroz, J. High Energy Phys. 04 (2019) 129.
[36] W. Grimus, L. Lavoura, and B. Radovčić, Phys. Lett. B **674**, 117 (2009).
[37] I. P. Ivanov, Phys. Rev. D **77**, 015017 (2008).
[38] G. 't Hooft, Nucl. Phys. **B79**, 276 (1974).
[39] A. M. Polyakov, JETP Lett. **20**, 194 (1974).
[40] H. B. Nielsen and P. Olesen, Nucl. Phys. **B61**, 45 (1973).
[41] R. A. Battye and D. G. Viatic, Phys. Lett. B **823**, 136730 (2021).